

**Fe<sub>3</sub>O<sub>4</sub>@SiO<sub>2</sub>-OSO<sub>3</sub>H NANOCOMPOSITE AS AN EFFICIENT CATALYST FOR THE PREPARATION OF TRICARBOXAMIDES****Mohammad Ali Ghasemzadeh\***

Department of Chemistry, Qom Branch, Islamic Azad University – Qom, I. R., Iran

Recebido em 29/04/2016 aceito em 07/07/2016, publicado na web em 31/08/2016

In this research a highly efficient one-pot preparation of tricarboxamide derivatives via five-component reactions of isocyanides, aldehydes Meldrum's acid and 2equiv. of amines have been developed in the presence of Fe<sub>3</sub>O<sub>4</sub>@SiO<sub>2</sub>-OSO<sub>3</sub>H nanocomposite. Nano-Fe<sub>3</sub>O<sub>4</sub> encapsulated-silica particles bearing sulfonic acid was readily recovered using an external magnet and could be reused several times without significant loss of reactivity. The catalyst was fully characterized by VSM, FT-IR, SEM, XRD, EDX and TEM analysis.

Keywords: Fe<sub>3</sub>O<sub>4</sub>@SiO<sub>2</sub>-OSO<sub>3</sub>H; Magnetite; Nanocomposite; Multi-component reaction; Core-shell; Tricarboxamide.

**INTRODUCTION**

Recently, to decrease waste and atom economy in the using raw materials, the purpose of technology and science has been modified toward more environmentally friendly, reusable catalysts and sustainable resources.<sup>1</sup> During the last decades, magnetic nanoparticles (MNPs) have been intensively investigated because of their broad applications such as ferrofluids, digital media recording, targeted drug delivery, magnetic hyperthermia, magnetic resonance imaging, etc.<sup>2,3</sup>

Magnetite Fe<sub>3</sub>O<sub>4</sub> nanoparticles (Fe<sub>3</sub>O<sub>4</sub> NPs) as a class of nano-sized materials have received great attention due to their wide range of usages in various fields such as medical applications, drug delivery, remediation, catalyst, industry.<sup>4-6</sup> The salient and significant property of magnetite nanoparticles is simple and facile separation of these catalysts from the reaction mixture using an external magnet. Coating magnetite nanoparticles with an amorphous silica layer is a useful and important approach in the growth of magnetite nanoparticle in various fields.<sup>7</sup> Silica shell in nanostructures is chemically inert and has high stability against aggregation. In addition, the existing of silanol parts on the surfaces can easily be functionalized via the appropriate surface modifications which causing to attach of different functionalities.<sup>8</sup> Furthermore, silanol groups on the surfaces of nanoparticles cause to protect of the related core toward oxidation and also various groups including guanidine,<sup>9</sup> proline,<sup>10</sup> sulfamic acid<sup>11</sup> and sulfonic acid<sup>12</sup> can attach to the outer shell.

In recent years, nano-Fe<sub>3</sub>O<sub>4</sub> encapsulated-silica particles bearing sulfonic acid (Fe<sub>3</sub>O<sub>4</sub>@SiO<sub>2</sub>-OSO<sub>3</sub>H) nanocomposites were applied as an effective nanocatalyst in the synthesis of 1,8-dioxo-octahydroanthene,<sup>13</sup> indazolo[2,1-b]phthalazine-triones and pyrazolo[1,2-b]phthalazine-diones,<sup>14</sup> functionalized pyrimido[4,5-b]quinolines and indeno fused pyrido[2,3-d]pyrimidines<sup>15</sup> and 3,4-dihydropyrimidinones/thiones.<sup>16</sup>

The multi-component coupling reactions (MCRs) are emerging as a valuable versatile for affording diverse organic structures for potential applications in medicinal and pharmaceutical chemistry.<sup>17</sup> MCRs often adapt to the goals of green chemistry connected to economy of reaction approaches as well as the many particular principles of favorable chemical transformations.<sup>18-20</sup> Due to of their benefits such as facile performance, environmentally friendly, fast and atom economic, MCRs interested great attention related to combinatorial chemistry.<sup>21</sup>

Tricarboxamide derivatives are a class of nitrogen heterocyclic compounds which have significant and well-reported biological activities that include neuroprotective,<sup>22</sup> anti-diabetic,<sup>23</sup> anti-bacterial,<sup>24</sup> anti-carcinogenic<sup>25</sup> and anti-tumor activities.<sup>26</sup>

Therefore, the importance of these constitutions has prompted researchers to develop more efficient pathways for the synthesis of these heterocycles compounds due to their significant biological and pharmaceutical properties.

In continuation of our attempts on using heterogeneous nanocatalysts in multi-component reactions,<sup>27-31</sup> herein we describe an efficient synthesis of functionalized tricarboxamide derivatives via five-component condensation reactions of isocyanides, aldehydes, Meldrum's acid and amines in the presence of magnetic Fe<sub>3</sub>O<sub>4</sub>@SiO<sub>2</sub>-OSO<sub>3</sub>H nanocomposites as catalyst under solvent-free conditions.

**EXPERIMENTAL****General**

Chemicals were purchased from the Sigma-Aldrich and Merck in high purity. All melting points are uncorrected and were determined in capillary tube on Boetius melting point microscope.<sup>1</sup>H NMR and <sup>13</sup>C NMR spectra were obtained on Bruker 400 MHz spectrometer with DMSO-*d*<sub>6</sub> as solvent using TMS as an internal standard. FT-IR spectrum was recorded on Magna-IR, spectrometer 550. The elemental analyses (C, H, N) were obtained from a Carlo ERBA Model EA 1108 analyzer. Powder X-ray diffraction (XRD) was carried out on a Philips diffractometer of X'pert Company with mono chromatized Cu K $\alpha$  radiation ( $\lambda = 1.5406 \text{ \AA}$ ). Microscopic morphology of products was visualized by SEM (LEO 1455VP). The mass spectra were recorded on a Joel D-30 instrument at an ionization potential of 70 eV. Transmission electron microscopy (TEM) was performed with a Jeol JEM-2100UHR, operated at 200 kV. Magnetic properties were obtained on a BHV-55 vibrating sample magnetometer (VSM) made by MDK-I.R.Iran. The compositional analysis was done by energy dispersive analysis of X-ray (EDX, KeveX, Delta Class I).

**Preparation of Fe<sub>3</sub>O<sub>4</sub> nanoparticles**

Fe<sub>3</sub>O<sub>4</sub> nanoparticles were prepared according to the procedure reported by Zhang *et al.*<sup>32</sup> To a solution of FeCl<sub>2</sub>·4H<sub>2</sub>O (2.5 g) and FeCl<sub>3</sub>·6H<sub>2</sub>O (6 g) in 30 mL deionized water was added dropwise 1.0 mL of concentrated hydrochloric acid at room temperature. The solution was added in to 300 mL of 1.5 mol L<sup>-1</sup> NaOH and then the solution

\*e-mail: Ghasemzadeh@qom-iau.ac.ir

was stirred vigorously at 80 °C until precipitation. Afterwards, the prepared magnetic nanoparticles were separated magnetically, washed with deionized water and then dried at 70 °C for 8 h.

#### Preparation of $Fe_3O_4@SiO_2$ nanocomposite

The core-shell  $Fe_3O_4@SiO_2$  nanocomposite were prepared according to the previously reported method.<sup>33</sup> Briefly 1g of  $Fe_3O_4$  nanoparticles was treated with 0.5 mol L<sup>-1</sup> HCl aqueous solution (25 mL) by sonication. After the treatment for 10 min, The magnetite particles were separated and washed with deionized water, and then homogeneously dispersed in the mixture of ethanol (60 mL), deionized water (100 mL) and concentrated ammonia aqueous solution (10 mL, 28 wt.%), followed by the addition of tetraethylorthosilicate (TEOS, 0.22 g, 0.144 mmol). After stirring at room temperature for 2 h, the  $Fe_3O_4@SiO_2$  nanocomposite were separated using an external magnet and washed with ethanol and water.

#### Preparation of $Fe_3O_4@SiO_2-OSO_3H$ nanocomposite

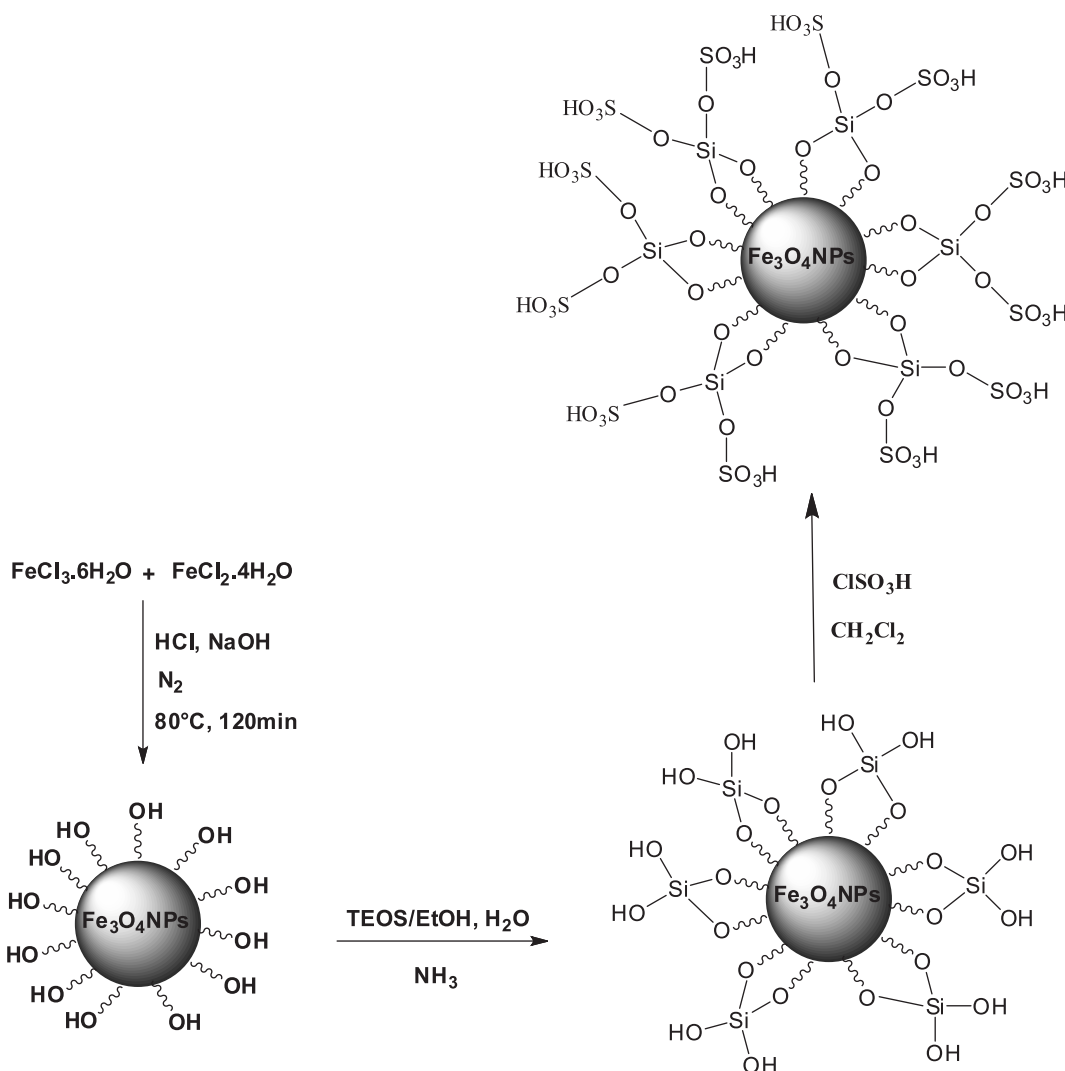
$Fe_3O_4@SiO_2-SO_3H$  MNPs were prepared according to a previously reported procedure by Kiasat and Davarpanah (Scheme 1).<sup>14</sup> A suction flask equipped with a constant-pressure dropping funnel. The gas outlet was connected to a vacuum system through an adsorbing solution of alkali trap. Firstly,  $Fe_3O_4@SiO_2$  (1 g) was added

to the flask and dispersed in dry  $CH_2Cl_2$  (10 ml) by ultrasonic for 30 min. Subsequently, chlorosulfonic acid (1 ml) was added drop-wise to a cooled (ice-bath) solution of  $Fe_3O_4@SiO_2$  (1 g) over a period of 30 min at room temperature. After completion of the addition, the mixture was stirred for a further 6 h until to allow for the complete dissipation of HCl from the reaction vessel. The resulted MNPs were separated using an external magnet and washed with ethanol and water before been dried in an oven at 70 °C to give  $Fe_3O_4@SiO_2-OSO_3H$  as a brown powder.

#### General procedure for the preparation of tricarboxamide derivatives

A mixture of isocyanide (1 mmol), aromatic aldehyde (1 mmol), Meldrum's acid (1 mmol), aromatic amine (2 mmol) and  $Fe_3O_4@SiO_2-OSO_3H$  nanocomposite (0.003 g) were heated in a sealed tube at 50 °C for appropriate times. Progress of the reaction was continuously monitored by TLC. After completion of the reaction, the mixture was cooled to room temperature and then was dissolved in methanol and then the nanocatalyst was separated using an external magnet. The solvent was evaporated under vacuum and the solid obtained recrystallized from EtOH to afford the pure tricarboxamides.

All of the products were characterized and identified with m.p., <sup>1</sup>H NMR, <sup>13</sup>C NMR and FT-IR spectroscopy techniques.



Scheme 1. Preparation steps of sulfonic acid-functionalized magnetite  $Fe_3O_4$  nanocomposite

## Spectral data of new compounds

*N*<sup>2</sup>-cyclohexyl-2-(4-fluorophenyl)-*N*<sup>1</sup>,*N*<sup>1</sup>-diphenylethane-1,1,2-tricarboxamide (**5f**): White solid; m.p 303-304 °C; FT- IR (KBr): 3314 (NH), 3291 (NH), 1673 (CO), 1615 (C=C), 1462 (C=C) cm<sup>-1</sup>; <sup>1</sup>H NMR (400 MHz, DMSO-*d*<sub>6</sub>) δ/ppm : 0.99-1.32 (m, 10 H, 5CH<sub>3</sub>), 3.27 (m, 1H, NCH), 4.01 (d, 1H, CH), 4.11 (d, 1H, CH), 6.91-7.63 (m, 14H, Ar), 8.41 (bs, 1H, NH), 10.12 (s, 2H, 2NH); <sup>13</sup>C NMR (100 MHz, DMSO-*d*<sub>6</sub>) δ/ppm : 173.1 (C=O), 169.4 (C=O), 149.1, 147.9, 144.6, 143.2, 131.3, 127.4, 121.2, 118.1, 64.3, 52.1, 48.1, 31.5, 30.4, 27.8. MS (EI) (*m/z*): 487 (M<sup>+</sup>); Anal. Calcd. mass fraction of elements, w/% for C<sub>29</sub>H<sub>30</sub>FN<sub>3</sub>O<sub>3</sub> (*M<sub>r</sub>* = 487.23) are: C 71.44; H 6.20; N 8.62; Found: C 71.32; H 6.26; N 8.69.

2-(4-cyanophenyl)-*N*<sup>2</sup>-cyclohexyl-*N*<sup>1</sup>,*N*<sup>1</sup>-diphenylethane-1,1,2-tricarboxamide (**5g**): White solid; m.p 312-315 °C; FT- IR (KBr): 3325 (NH), 3286 (NH), 2211 (CN), 1668 (CO), 1584 (C=C), 1453 (C=C) cm<sup>-1</sup>; <sup>1</sup>H NMR (400 MHz, DMSO-*d*<sub>6</sub>) δ/ppm : 1.01-1.29 (m, 10 H, 5CH<sub>3</sub>), 3.31 (m, 1H, NCH), 4.03 (d, 1H, CH), 4.10 (d, 1H, CH), 6.95-7.42 (m, 14H, Ar), 8.38 (bs, 1H, NH), 10.09 (s, 2H, 2NH); <sup>13</sup>C NMR (100 MHz, DMSO-*d*<sub>6</sub>) δ/ppm : 172.8 (C=O), 168.1 (C=O), 149.2, 147.9, 145.1, 143.6, 131.3, 127.4, 120.8, 119.2, 116.5, 62.1, 51.9, 48.3, 30.8, 29.2, 27.6. MS (EI) (*m/z*): 494 (M<sup>+</sup>); Anal. Calcd. mass fraction of elements, w/% for C<sub>30</sub>H<sub>30</sub>N<sub>4</sub>O<sub>3</sub> (*M<sub>r</sub>* = 494.23) are: C 72.85; H 6.11; N 11.33; Found: C 72.97; H 6.16; N 11.19.

*N*<sup>2</sup>-(*tert*-butyl)-2-(4-fluorophenyl)-*N*<sup>1</sup>,*N*<sup>1</sup>-diphenylethane-1,1,2-tricarboxamide (**5m**): White solid; m.p 285-287 °C; FT- IR (KBr): 3303 (NH), 3278 (NH), 1675 (CO), 1606 (C=C), 1458 (C=C) cm<sup>-1</sup>; <sup>1</sup>H NMR (400 MHz, DMSO-*d*<sub>6</sub>) δ/ppm : 0.98-1.22 (s, 9 H, 3CH<sub>3</sub>), 3.87 (d, 1H, CH), 4.11 (d, 1H, CH), 7.07-7.64 (m, 14H, Ar), 8.27 (bs, 1H, NH), 10.23 (s, 2H, 2NH); <sup>13</sup>C NMR (100 MHz, DMSO-*d*<sub>6</sub>) δ/ppm : 176.2 (C=O), 172.5 (C=O), 151.2, 149.8, 144.1, 143.2, 131.1, 128.1, 120.7, 118.6, 64.1, 50.8, 42.9, 28.1. MS (EI) (*m/z*): 461 (M<sup>+</sup>); Anal. Calcd. mass fraction of elements, w/% for C<sub>27</sub>H<sub>28</sub>FN<sub>3</sub>O<sub>3</sub> (*M<sub>r</sub>* = 461.21) are: C 70.26; H 6.12; N 9.10; Found: C 70.42; H 5.98; N 9.03.

*N*<sup>2</sup>-(*tert*-butyl)-2-(4-cyanophenyl)-*N*<sup>1</sup>,*N*<sup>1</sup>-diphenylethane-1,1,2-tricarboxamide (**5n**): White solid; m.p 293-295 °C; FT- IR (KBr): 3341 (NH), 3291 (NH), 2216 (CN), 1678 (CO), 1603 (C=C), 1483 (C=C) cm<sup>-1</sup>; <sup>1</sup>H NMR (400 MHz, DMSO-*d*<sub>6</sub>) δ/ppm : 1.02-1.33 (m, 9 H, 3CH<sub>3</sub>), 3.91 (D, 1H, CH), 4.11 (d, 1H, CH), 6.98-7.53 (m, 14H, Ar), 8.22 (bs, 1H, NH), 10.14 (s, 2H, 2NH); <sup>13</sup>C NMR (100 MHz, DMSO-*d*<sub>6</sub>) δ/ppm : 171.1 (C=O), 168.4 (C=O), 148.8, 147.5, 145.1, 142.4, 129.1, 128.6, 123.7, 111.4, 115.1, 63.9, 51.1, 38.8, 28.2. MS (EI) (*m/z*): 468 (M<sup>+</sup>); Anal. Calcd. mass fraction of elements, w/%

for C<sub>28</sub>H<sub>28</sub>N<sub>4</sub>O<sub>3</sub> (*M<sub>r</sub>* = 468.22) are: C 71.78; H 6.02; N 11.96; Found: C 71.67; H 5.92; N 12.14.

## Recycling and Reusing of the Catalyst

After completion of the reaction, the obtained product was dissolved in methanol and then the nanocatalyst was separated by an external magnet, then the nanocatalyst were washed three to four times with methanol and ethyl acetate and then dried overnight in an oven at 50 °C. To investigate lifetime and level of recoverability of the Fe<sub>3</sub>O<sub>4</sub>@SiO<sub>2</sub>-OSO<sub>3</sub>H MNPs, the model study was carried out several times using recycled magnetite nanocomposite. The summarized results of Table 1 show that the recovered catalyst could be used for five successive runs with a slightly decreased in activity.

**Table 1.** Reusability of the Fe<sub>3</sub>O<sub>4</sub>@SiO<sub>2</sub>-OSO<sub>3</sub>H nanostructures in model study

Yield (%)				
First	Second	Third	Fourth	Fifth
95	95	92	89	87

## RESULTS AND DISCUSSION

In the initial experiments Fe<sub>3</sub>O<sub>4</sub>@SiO<sub>2</sub>-SO<sub>3</sub>H nanocomposites was prepared and characterized by EDX, SEM XRD, FT-IR VSM and TEM analysis.

The chemical purity of the samples as well as their stoichiometry was tested by EDX studies. The EDX spectrum given in Figure 1a shows the presence of Fe and O as the only elementary components of Fe<sub>3</sub>O<sub>4</sub> NPs. EDX spectrum Fe<sub>3</sub>O<sub>4</sub>@SiO<sub>2</sub> (Figure 1b) shows the elemental compositions are (Fe, O and Si) of core-shell nanocomposites. EDX spectrum of Fe<sub>3</sub>O<sub>4</sub>@SiO<sub>2</sub>-OSO<sub>3</sub>H (Figure 1c) shows the elemental compositions are (Fe, Si, O and S) of magnetic nanocomposites.

Scanning electron microscopy (SEM) is a useful tool for determining the size distribution, particles shape, and porosity. It has been a primary tool for characterizing the surface morphology and fundamental physical properties of the surface. According to Figure 2b, Fe<sub>3</sub>O<sub>4</sub>@SiO<sub>2</sub> nanocomposites still keep the morphological properties of Fe<sub>3</sub>O<sub>4</sub> (Figure 2a) except for a slightly larger particle size and smoother surface, while silica are uniformly coated on the Fe<sub>3</sub>O<sub>4</sub> particles to form silica shell compared to the Fe<sub>3</sub>O<sub>4</sub>@SiO<sub>2</sub>. The SEM image shown in Figure 2c demonstrates that Fe<sub>3</sub>O<sub>4</sub>@SiO<sub>2</sub>-OSO<sub>3</sub>H nanocomposite are nearly spherical with about 30 nm in size.

The structure of Fe<sub>3</sub>O<sub>4</sub> (a), Fe<sub>3</sub>O<sub>4</sub>@SiO<sub>2</sub> (b) and Fe<sub>3</sub>O<sub>4</sub>@SiO<sub>2</sub> sulfonic acid (c) were analyzed by X-ray diffraction (XRD)

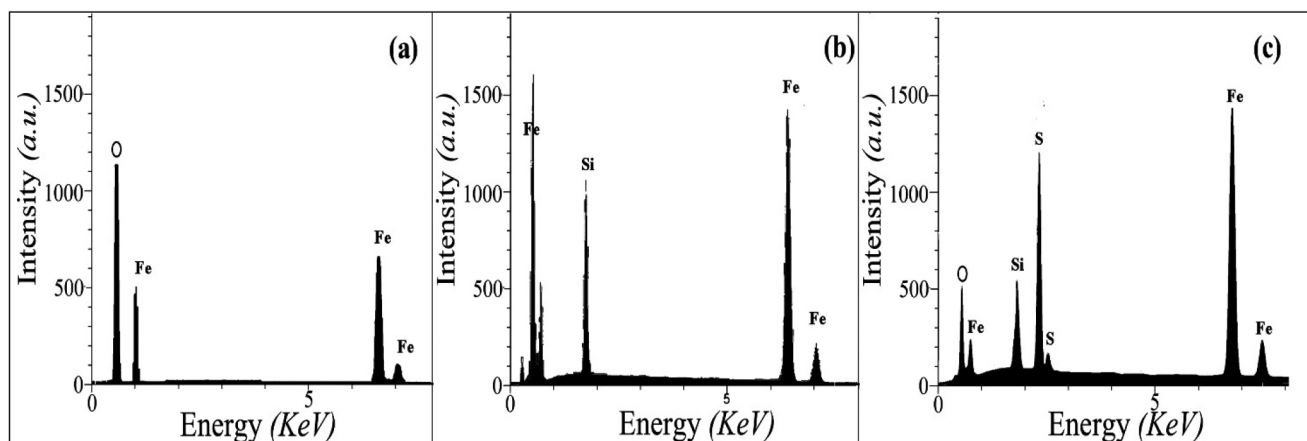


**Figure 1.** The EDX spectra of (a) Fe<sub>3</sub>O<sub>4</sub>, (b) Fe<sub>3</sub>O<sub>4</sub>@SiO<sub>2</sub> and (c) Fe<sub>3</sub>O<sub>4</sub>@SiO<sub>2</sub>-OSO<sub>3</sub>H MNPs

spectroscopy (Figure 3). XRD diagram of the bare  $\text{Fe}_3\text{O}_4$  NPs displayed patterns consistent with the patterns of spinel ferrites described in the literature (Figure 3).<sup>11</sup> The same peaks were observed in the both of the  $\text{Fe}_3\text{O}_4@SiO_2$  and  $\text{Fe}_3\text{O}_4@SiO_2$  sulfonic acid XRD patterns, indicating retention of the crystalline spinel ferrite core structure during the silica-coating process. The average MNPs core diameter of  $\text{Fe}_3\text{O}_4$ ,  $\text{Fe}_3\text{O}_4@SiO_2$  and  $\text{Fe}_3\text{O}_4@SiO_2$  sulfonic acid were calculated to be about 18, 25 and 32 nm, respectively from the XRD results by Scherrer's equation.

The FT-IR spectra of  $\text{Fe}_3\text{O}_4$  nanoparticles,  $\text{Fe}_3\text{O}_4@SiO_2$ , and  $\text{Fe}_3\text{O}_4@SiO_2$  sulfonic acid are shown in Figure 4. The FT-IR analysis of the  $\text{Fe}_3\text{O}_4@SiO_2$  and  $\text{Fe}_3\text{O}_4@SiO_2$  sulfonic acid exhibits two basic

characteristic peaks at  $\sim 3300\text{ cm}^{-1}$  (O–H stretching) and  $580\text{ cm}^{-1}$  (Fe–O vibration).<sup>34</sup> The band at  $1081\text{ cm}^{-1}$  comes from the Si–O–Si group. The presence of the sulfonyl group of  $\text{Fe}_3\text{O}_4@SiO_2$  sulfonic acid is confirmed by  $1217\text{ cm}^{-1}$  and  $1124\text{ cm}^{-1}$  bands, which were covered by a stronger absorption of Si–O bonds at  $1081\text{ cm}^{-1}$ .<sup>11</sup> A wide band at  $2500\text{--}3409\text{ cm}^{-1}$  is due to the stretching of OH groups in the  $\text{SO}_3\text{H}$ .

The magnetic properties of the uncoated magnetic iron oxide ( $\text{Fe}_3\text{O}_4$ ),  $\text{Fe}_3\text{O}_4@SiO_2$ , and  $\text{Fe}_3\text{O}_4@SiO_2\text{-SO}_3\text{H}$  were measured by vibrating sample magnetometer, VSM, at room temperature (Figure 5). In Figure 5, the hysteresis loops that are characteristic of superparamagnetic behavior can be clearly observed for all

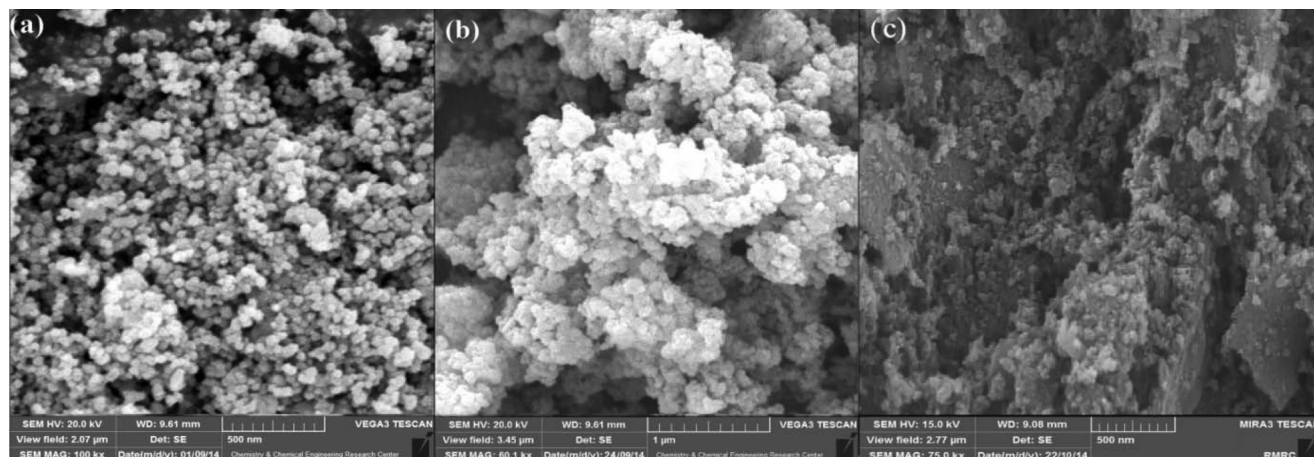


Figure 2. The SEM images of (a)  $\text{Fe}_3\text{O}_4$ , (b)  $\text{Fe}_3\text{O}_4@SiO_2$  and (c)  $\text{Fe}_3\text{O}_4@SiO_2\text{-OSO}_3\text{H}$  MNPs

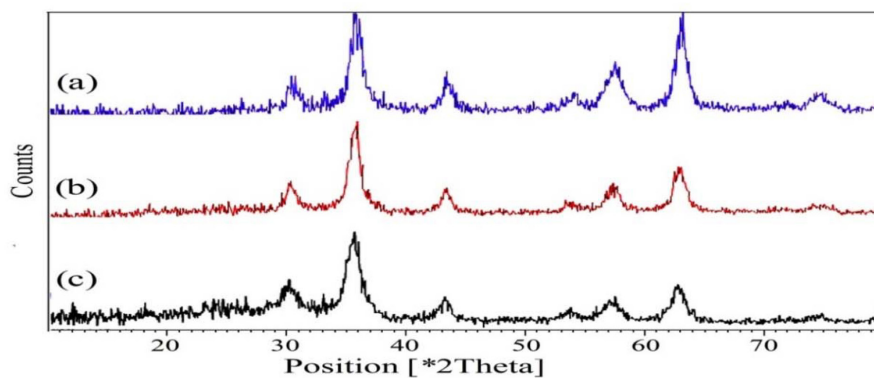


Figure 3. XRD patterns of (a)  $\text{Fe}_3\text{O}_4$ , (b)  $\text{Fe}_3\text{O}_4@SiO_2$  and (c)  $\text{Fe}_3\text{O}_4@SiO_2\text{-OSO}_3\text{H}$  MNPs

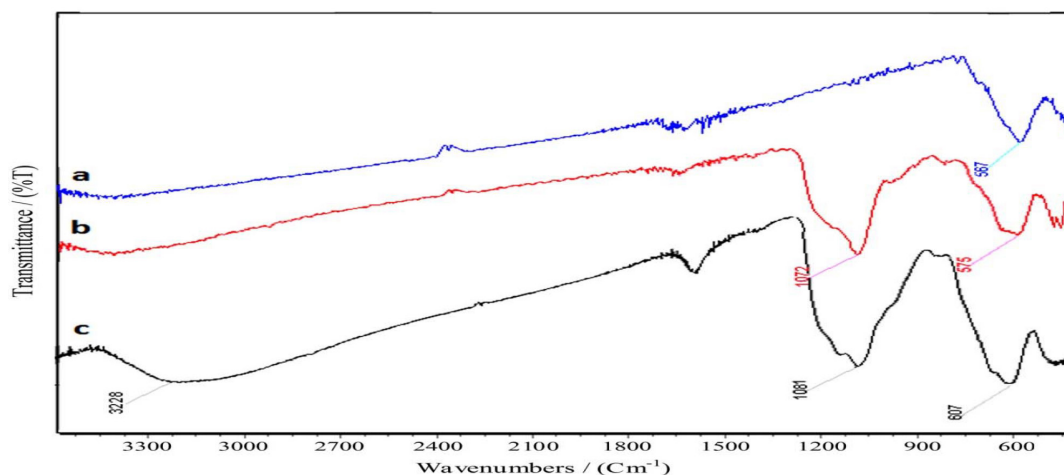


Figure 4. The FT-IR spectra of (a)  $\text{Fe}_3\text{O}_4$ , (b)  $\text{Fe}_3\text{O}_4@SiO_2$  and (c)  $\text{Fe}_3\text{O}_4@SiO_2\text{-OSO}_3\text{H}$  MNPs



the nanoparticles. Superparamagnetism is the responsiveness to an applied magnetic field without retaining any magnetism after removal of the applied magnetic field. From M versus H curves, the saturation magnetization value (M<sub>s</sub>) of uncoated Fe<sub>3</sub>O<sub>4</sub> NPs was found to be 48.12 emu g<sup>-1</sup>. For Fe<sub>3</sub>O<sub>4</sub>@SiO<sub>2</sub> and Fe<sub>3</sub>O<sub>4</sub>@SiO<sub>2</sub>-SO<sub>3</sub>H, the magnetization obtained at the same field were 38.16 and 35.82 emu g<sup>-1</sup>, respectively, lower than that of uncoated Fe<sub>3</sub>O<sub>4</sub>. These results indicated that the magnetization of Fe<sub>3</sub>O<sub>4</sub> decreased considerably with the increase of SiO<sub>2</sub> and SO<sub>3</sub>H. This is mainly attributed to the existence of nonmagnetic materials on the surface of the nanoparticles.

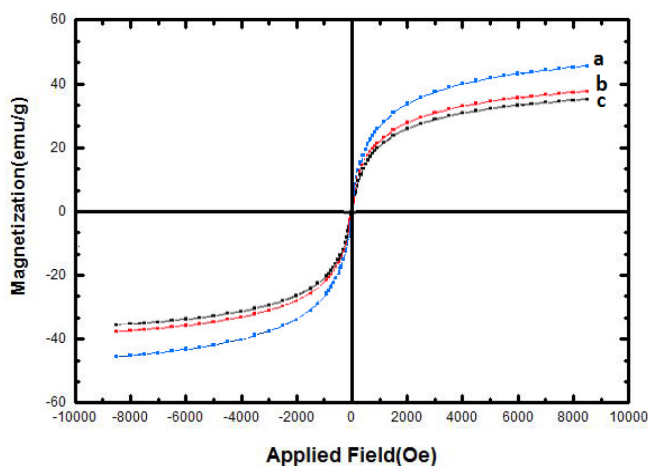


Figure 5. VSM magnetization curves of the (a) Fe<sub>3</sub>O<sub>4</sub>, (b) Fe<sub>3</sub>O<sub>4</sub>@SiO<sub>2</sub> and (c) Fe<sub>3</sub>O<sub>4</sub>@SiO<sub>2</sub>-OSO<sub>3</sub>H MNPs

The size and morphology of Fe<sub>3</sub>O<sub>4</sub>@SiO<sub>2</sub>-SO<sub>3</sub>H nanocomposites were analyzed by Transmission electron microscopy (TEM) (Figure 6). The results show that these nanocatalysts consist of spherical particles with the crystallite size about 30 nm, confirming the results calculated from Scherrer's formula based on the XRD pattern.

Initially, to optimize the reaction conditions, the reaction of 4-bromobenzaldehyde, Meldrum's acid, *tert*-butyl isocyanide and aniline was selected as a model reaction (Scheme 2).

The reaction conditions were optimized on the basis of the solvent, catalyst, and different temperatures for synthesis of tricarboxamide (5a).

To show the advantage of the current approach in comparison to other catalysts, the model reaction was carried out using various nanocatalysts such as ZnO, MgO, CuO, AgI, Co<sub>3</sub>O<sub>4</sub> and Fe<sub>3</sub>O<sub>4</sub>@SiO<sub>2</sub>-SO<sub>3</sub>H. From the results provided in Table 2, it was clear that nano-Fe<sub>3</sub>O<sub>4</sub> encapsulated-silica particles bearing sulfonic acid afforded the corresponding tricarboxamide (5a) in excellent yield and short reaction time (60 min in 95 % yield).

Table 2. The model reaction catalyzed by various catalysts.

Entry	Catalyst	Time (min)	Yield (%) <sup>b</sup>
1	ZnO	150	45
2	MgO	180	trace
3	CuO	150	40
4	AgI	100	70
5	Co <sub>3</sub> O <sub>4</sub>	90	75
6	Fe <sub>3</sub> O <sub>4</sub> @SiO <sub>2</sub> -OSO <sub>3</sub> H	60	95

<sup>a</sup>The reaction was carried out under solvent-free conditions at 50°C. <sup>b</sup>Isolated yields

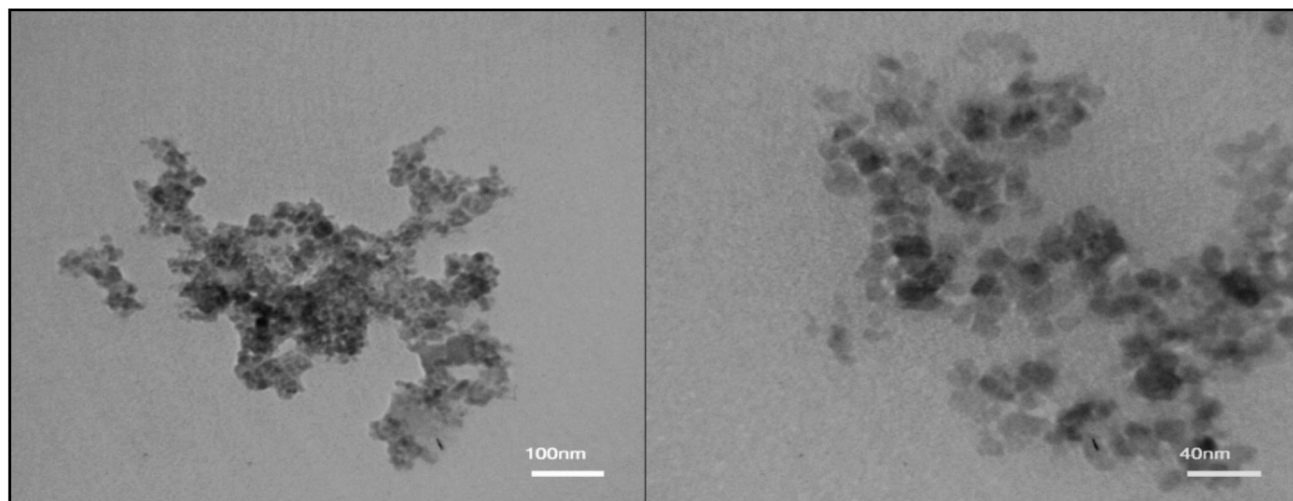
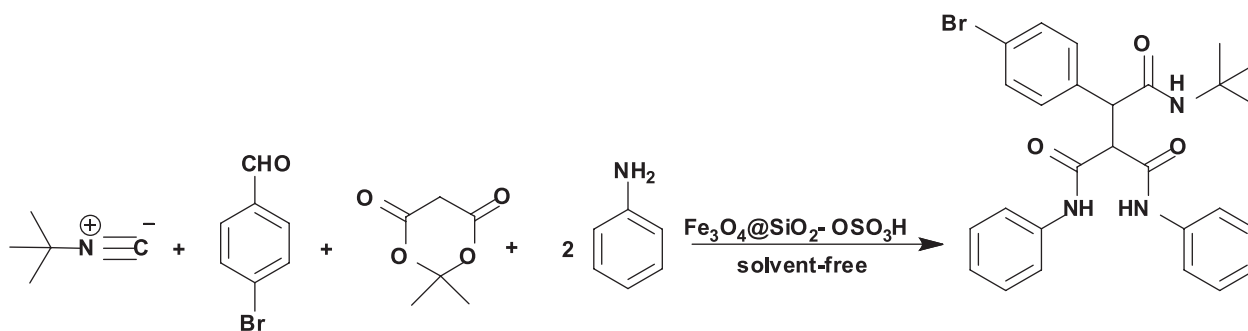


Figure 6. TEM images of Fe<sub>3</sub>O<sub>4</sub>@SiO<sub>2</sub>-OSO<sub>3</sub>H MNPs



Scheme 2. The model study for the synthesis of tricarboxamide (5a)

During the optimization of reaction conditions the influence of solvent was studied when the model reaction was carried out using  $\text{Fe}_3\text{O}_4@\text{SiO}_2\text{-OSO}_3\text{H}$  MNPs by different solvents and also solvent-free conditions.

We found that the best result was obtained when the reaction was carried out under solvent-free conditions at 50 °C. Increasing temperature showed unsatisfactory effect on the yield and reaction time (Table 3).

The reaction conditions were also investigated with different catalyst loading, revealing that 0.003 g of the catalyst provided the best results in terms of reaction time, economy of catalyst charge,

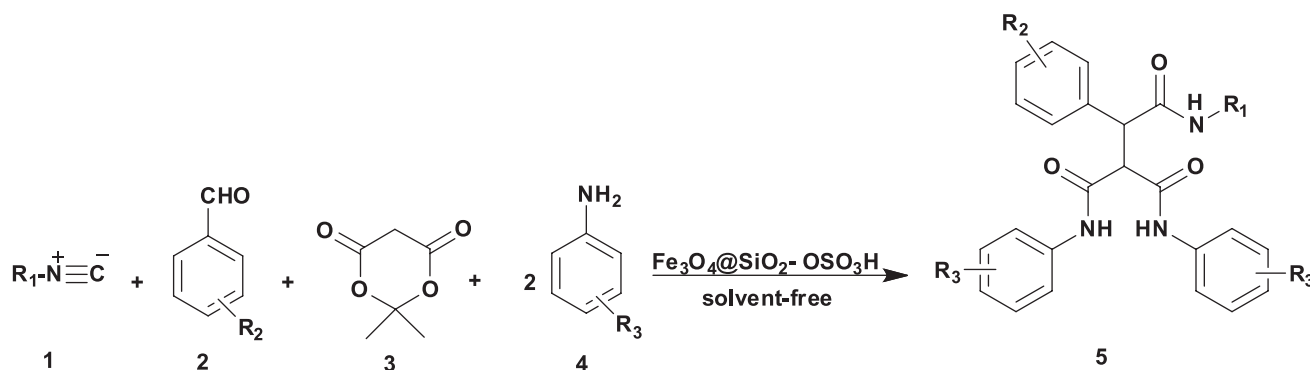
and reaction yield (Table 3, entry 5). As shown in Table 3 increasing the amount of catalyst does not improve the yield of the product any further, whereas decreasing the amount of catalyst leads to decrease in the product yield. Hence, the optimum concentration of  $\text{Fe}_3\text{O}_4@\text{SiO}_2\text{-OSO}_3\text{H}$  was chosen 0.003 g in the model reaction.

To study the scope and limitations of multi-component synthesis of tricarboxamide, we next utilized a diversity of aldehydes and amines to investigate five-component reactions under the optimized conditions (Scheme 3). As shown in Table 4, aldehydes with both electron-withdrawing and electron donating groups were effectively produced the corresponding products. In addition aryl amines with

**Table 3.** Effect of solvent, temperature and catalyst amounts in the model study

Entry	Catalyst (g)	Solvent	T °C	Time (min)	Yield (%) <sup>a</sup>
1	0.01	Solvent-free	25	120	55
2	0.01	Solvent-free	50	60	95
3	0.01	Solvent-free	80	60	45
4	0.005	Solvent-free	50	60	95
<b>5</b>	<b>0.003</b>	<b>Solvent-free</b>	<b>50</b>	<b>60</b>	<b>95</b>
6	0.001	Solvent-free	50	90	70
7	0.003	EtOH (r.t.)	25	180	80
8	0.003	$\text{CH}_2\text{Cl}_2$ (r.t.)	25	300	45
9	0.003	$\text{CH}_3\text{CN}$ (r.t.)	25	240	65
10	0.003	$\text{H}_2\text{O}$ (r.t.)	25	360	35

<sup>a</sup>Isolated yields.



**Scheme 3.** Preparation of tricarboxamides catalyzed by  $\text{Fe}_3\text{O}_4@\text{SiO}_2\text{-OSO}_3\text{H}$  nanocomposite

**Table 4.** Preparation of tricarboxamides catalyzed by  $\text{Fe}_3\text{O}_4@\text{SiO}_2\text{-OSO}_3\text{H}$  NPs

Entry	Aldehyde ( $\text{R}_2$ )	Aniline ( $\text{R}_3$ )	Isocyanide	Product <sup>b</sup>	Time (min)	Yield (%) <sup>c</sup>
1	4-Br	H	cyclohexyl	<b>5a</b>	60	95
2	H	H	cyclohexyl	<b>5b</b>	70	88
3	4- $\text{NO}_2$	H	cyclohexyl	<b>5c</b>	50	93
4	4- $\text{NO}_2$	4-OMe	cyclohexyl	<b>5d</b>	45	96
5	4-Me	H	cyclohexyl	<b>5e</b>	70	86
6	4-F	H	cyclohexyl	<b>5f</b>	65	90
7	4-CN	H	cyclohexyl	<b>5g</b>	60	92
8	4-Br	H	tert-butyl	<b>5h</b>	50	95
9	H	H	tert-butyl	<b>5i</b>	60	90
10	4- $\text{NO}_2$	H	tert-butyl	<b>5j</b>	45	95
11	4- $\text{NO}_2$	4-OMe	tert-butyl	<b>5k</b>	45	94
12	4-Me	H	tert-butyl	<b>5l</b>	65	89
13	4-F	H	tert-butyl	<b>5m</b>	55	95
14	4-CN	H	tert-butyl	<b>5n</b>	50	93

<sup>a</sup>Reaction conditions: aromatic aldehyde, aromatic amine, isocyanide and Meldrum's acid (1:2:1:1 molar ratio) using 0.003 g of  $\text{Fe}_3\text{O}_4@\text{SiO}_2\text{-OSO}_3\text{H}$  MNPs under solvent-free conditions at 50 °C. <sup>b</sup>Compounds **5f**, **5g**, **5m** and **5n** are new products. <sup>c</sup>Isolated yield.

various substituents afforded tricarboxamide derivatives in excellent yields and short reaction times. Comparison between tert-butyl isocyanide and cyclohexyl isocyanide shows that multi-component reactions of isocyanides, aldehydes Meldrum's acid and amines was smoothly proceed using tert-butyl isocyanide.

## CONCLUSIONS

In summary, we have described a highly effective, mild and green approach for the preparation of tricarboxamide using Fe<sub>3</sub>O<sub>4</sub>@SiO<sub>2</sub>-OSO<sub>3</sub>H nanocomposites under solvent-free conditions at 50 °C. The products were obtained in excellent yields and short reaction times via one-pot pseudo-five component reactions of isocyanides, aldehydes Meldrum's acid and 2 equiv. of amines. The salient properties of the applied nanocatalyst are simple work-up procedure, ease of separation, and recyclability of the magnetic nanocatalyst.

## ACKNOWLEDGEMENTS

This work is funded by the Research Affairs Office of the Islamic Azad University, Qom Branch, Qom, I. R. Iran [grant number 2014-13929].

## REFERENCES

- Zhang, Y.; Zhao, Y.; Xia, C.; *J. Mol. Catal. A: Chem.* **2009**, *306*, 107.
- Raj, K.; Moskowitz, R.; *J. Magn. Magn. Mater.* **1990**, *85*, 233.
- Pankhurst, Q. A.; Connolly, J.; Jones, S. K.; Dobson, J.; *J. Phys. D: Appl. Phys.* **2003**, *36*, R167.
- Lu, A.-H.; Salabas, E. L.; Schuth, F.; *Angew. Chem. Int. Ed.* **2007**, *46*, 1222.
- Perez, J. M.; *Nat. Nanotechnol.* **2007**, *2*, 535.
- Sun, S. H.; Murray, C. B.; Folks, D. L.; Moser, A.; *Science* **2000**, *287*, 1989.
- Kim, J.; Lee, J. E.; Lee, J.; Yu, J. H.; Kim, B. C.; An, K.; Hwang, Y.; Shin, C.-H.; Park, Je-G.; Kim, J.; Hyeon, T.; *J. Am. Chem. Soc.* **2006**, *128*, 688.
- Shen, H.; Chen, J.; Dai, H.; Wang, L.; Hu, M.; Xia, Q.; *Ind. Eng. Chem. Res.* **2013**, *52*, 12723.
- Atashkar, B.; Rostami, A.; Tahmasbi, B.; *Catal. Sci. Technol.* **2013**, *21*, 44.
- Yang, H.; Li, S.; Wang, X.; Zhang, F.; Zhong, X.; Dong, Z.; Ma, J.; *J. Mol. Catal. A: Chem.* **2012**, *363–364*, 404.
- Kassae, M. Z.; Masrouri, H.; Movahedi, F.; *Appl. Catal. A: Gen.* **2011**, *395*, 28.
- Nemati, F.; Heravi, M. M.; Saeeedirad, R.; *Chin. J. Catal.* **2012**, *33*, 1825.
- Naeimi, H.; Nazifi, Z. S.; *J. Nanopart. Res.* **2013**, *15*, 2026.
- Kiasat, A. R.; Davarpanah, J.; *J. Mol. Catal. A: Chem.* **2013**, *373*, 46.
- Nemati, F.; Saeeedirad, R.; *Chin. Chem. Lett.* **2013**, *24*, 370.
- Kiasat, A. R.; Davarpanah, A.; *Res. Chem. Intermed.* **2015**, *41*, 2991.
- Ulaczyk-Lesanko, A.; Hall, D. G.; *Curr. Opin. Chem. Biol.* **2005**, *9*, 266.
- Domling, A.; Ugi, I.; *Angew. Chem. Int. Ed.* **2000**, *39*, 3168.
- Zhang, X. N.; Li, Y. X.; Zhang, Z. H.; *Tetrahedron*, **2011**, *67*, 7426.
- Mohammadi Ziarani, G.; Moradi, R.; Lashgari, N.; Badiei, A.; Abolhasani Soorki, A.; *Quim. Nova* **2015**, *38*, 1167.
- Schätz, A.; Reiser, O.; Stark, W. J.; *Chem. Eur. J.* **2010**, *16*, 8950.
- Faden, A. I.; Movsesyan, V. A.; Knobloch, S. M.; Ahmed, F.; Cernak, I.; *Neuropharmacology*, **2005**, *49*, 410.
- Tang, X.; Fan, L.; Yu, H.; Liao, Y.; Yang, D.; *Chin. J. Org. Chem.* **2009**, *29*, 595.
- Strom, K.; Sjogren, J.; Broberg, A.; Schnurer, J.; *Appl. Environ. Microbiol.* **2002**, *68*, 4322.
- Cui, C.; Kakeya, B. H.; Osada, H.; *Tetrahedron* **1997**, *53*, 59.
- Wang, J. L.; Liu, D.; Zheng, Z. J.; *Proc. Natl. Acad. Sci. U.S.A.* **2000**, *97*, 7124.
- Safaei-Ghomi, J.; Taheri, M.; Ghasemzadeh, M. A.; *Org. Prep. Proced. Int.* **2010**, *42*, 485.
- Ghasemzadeh, M. A.; Safaei-Ghomi, J.; *J. Chem. Res.* **2014**, *38*, 313.
- Ghasemzadeh, M. A.; Abdollahi-Basir, M. H.; Babaei, M.; *Green Chem. Lett. Rev.* **2015**, *8*, 40.
- Ghasemzadeh, M. A.; Safaei-Ghomi, J.; Zahedi, S.; *J. Serb. Chem. Soc.* **2013**, *78*, 769.
- Ghasemzadeh, M. A.; Safaei-Ghomi, J.; *Acta Chim. Slov.* **2015**, *62*, 103.
- Lu, H. Y.; Yang, S. H.; Deng, J.; Zhang, Z. H.; *Aust. J. Chem.* **2010**, *63*, 1290.
- Xu, X. Q.; Deng, C. H.; Gao, M. X.; Yu, W. J.; Yang, P. Y.; Zhang, X. M.; *Adv. Mater.* **2006**, *18*, 3289.
- Lin, Y.; Chen, H.; Lin, K.; Chen, B.; Chiou, C.; *J. Environ. Sci.* **2011**, *23*, 44.